

## Corrosion Inhibition of Titanium in Hydrochloric Acid containing Na<sub>2</sub>MoO<sub>4</sub>

Junying Hu<sup>\*</sup>, Longjun Chen, Xiankang Zhong, Siyu Yu, Zhi Zhang, Dezhi Zeng, Taihe Shi

State Key Laboratory of Oil and Gas Reservoir Geology and Exploitation, School of Oil and Natural Gas Engineering, Southwest Petroleum University, Chengdu 610500, China

\*E-mail: [hujunying01@yeah.net](mailto:hujunying01@yeah.net)

Received: 27 May 2017 / Accepted: 19 July 2017 / Published: 12 September 2017

The corrosion inhibition behaviors and mechanisms of Na<sub>2</sub>MoO<sub>4</sub> for Ti in 15wt% HCl-acidizing fluid used in natural gas exploitation were studied via potentiodynamic polarization, electrochemical impedance spectroscopy (EIS) and Mott–Schottky techniques. The results show that the MoO<sub>4</sub><sup>2-</sup> plays a significant role in the formation and stability of the passive film on Ti surface. As the concentration of MoO<sub>4</sub><sup>2-</sup> increases to 0.01 wt%, the hydrogen evolution reaction (cathodic process) is apparently inhibited, and the anode process changes from active-passivation state to passivation state.

**Keywords:** Corrosion; Acidizing fluid; Ti; Na<sub>2</sub>MoO<sub>4</sub>

### 1. INTRODUCTION

Ti and its alloys are widely used in chemical, medical implant materials, aerospace, and other fields due to their unique physical and chemical properties, including light weight, weldability, excellent chemical stability and strong passivation capability in highly corrosive environment [1-6]. It is well known that it is extremely corrosive for the materials used in the wells with high temperature and high pressure. Ti alloys have already shown a great potential to be used as tubing or other downhole tools under such conditions. For example, it is recently reported that Ti alloy has been successfully used as tubing in Yuanba gas well which is a super-deep gas well with high content of H<sub>2</sub>S, located in Langzhong, Sichuan, China [7].

Although Ti alloys show an excellent anti-corrosion performance in H<sub>2</sub>S environment, they have a poor corrosion resistance in acidizing fluid such as hydrochloric acid and hydrofluoric acid [8-12]. Therefore, the inhibition of Ti alloys in acidizing fluid is of great importance for their use in oil and gas field. The use of inhibitors is one of the most common methods for inhibition of metal and

alloys used in the production of oil and gas field. For Ti alloys, a series of inhibitors have been developed, such as  $\text{Fe}^{3+}$ ,  $\text{Cu}^{2+}$ ,  $\text{MoO}_4^{2-}$  and some organic compounds [13-16]. It is reported that molybdate can effectively inhibit the corrosion of Ti and Ti alloys in most conditions. For example, Mogada and co-workers studied the inhibition of Ti-6Al-4V alloy in the sulfuric and hydrochloric acid solutions using molybdate. It is found that a highly protective passive film on the Ti alloy can be formed in the solution containing molybdate [14]. Cheng and co-workers also found that the addition of molybdate in boiling sulphuric acid with concentrations higher than 1 mM could greatly reduce the corrosion rate to a negligible value [17].

Although extensive work has been conducted on the effect of molybdate on the inhibition of Ti and Ti alloys, the inhibition mechanism of molybdate on Ti and Ti alloys in acidizing fluid in oil and gas production is seldom studied. To clarify the inhibition mechanism, the electrochemical technique is usually employed, which can provide in depth insight in mechanism analysis [18-20]. In this work, potentiodynamic polarization, electrochemical impedance spectroscopy (EIS), and Mott-Schottky analysis, combined with scanning electron microscopy (SEM) techniques, were used to study inhibition behaviors and mechanisms of  $\text{Na}_2\text{MoO}_4$  on the corrosion of Ti in hydrochloric acid solution.

## 2. EXPERIMENTAL

### 2.1. Sample and solution

Samples which were cut from a commercial pure Ti pipe (ZS Advanced Material Co., Ltd., China) were used in this work. All the samples were evenly abraded by sand paper with 600 and 800 grit numbers, sequentially, and then cleaned in an ultrasonic bath with petroleum ether. Samples then were taken out and dried by nitrogen gas and immediately used for measurement. The 15 wt% HCl solution with different contents (0.01, 0.05, 0.1 and 0.3 wt%) of  $\text{Na}_2\text{MoO}_4$  was prepared from deionized water and analytical grade reagents. The test solution was deoxygenated with a continuous  $\text{N}_2$  gas flow purge. All the experiments were carried out at 40 °C and atmospheric pressure.

### 2.2. Electrochemical tests

The electrochemical tests, including polarization curves and electrochemical impedance spectroscopy (EIS), were conducted using a CS 350 electrochemical workstation (Wuhan Corrtest Instruments Corp. Ltd., China). A conventional three-electrode configuration was employed in the tests where a saturated calomel electrode (SCE) was used as a reference electrode and Pt sheet was used as a counter electrode. A cylindrical Ti sample used as working electrode was embedded in an epoxy cylinder where the exposed surface area is 0.4  $\text{cm}^2$ . Polarization curves were performed by shifting the potential from -0.5 V (vs. Opening Circuit Potential, OCP) to +4.5 V (vs. OCP) with a scanning rate of 0.5 mV/s. The inhibition efficiency ( $\eta_i$ ) can be calculated according to the following equation:

$$\eta_i(\%) = \frac{I_{0,\text{corr}} - I_{\text{corr}}}{I_{0,\text{corr}}} \times 100\% \quad (1)$$

where  $I_{0,\text{corr}}$  and  $I_{\text{corr}}$  represent the corrosion current densities of Ti in the blank solution and the  $\text{Na}_2\text{MoO}_4$  containing solution, respectively.

The EIS measurements were performed at OCP with a peak-to-peak 5 mV sinusoidal perturbation at the frequency from 10000 Hz to 10 mHz, with 12 points per decade. Z-view software was used to analyze the EIS data. To investigate the properties of passive film on Ti, Mott-Schottky curves of Ti were measured in different solution. Mott-Schottky tests were performed by shifting the potential from -0.6 V (vs. OCP) to +0.5 V (vs. OCP) with a scanning rate of 1mV per step at 1 kHz. Each type of electrochemical measurements was repeated at least three times.

### 2.3. Characterization of surface morphologies and composition

The surface morphologies of samples were observed by scanning electronic microscopy (SEM, Phillips Quanta 200, America) and the surface composition was also detected by energy dispersive spectroscopy.

## 3. RESULTS AND DISCUSSION

### 3.1. Open circuit potential (OCP)

The OCP vs. time curves of Ti in deoxygenated 15 wt% HCl solution containing different contents of  $\text{Na}_2\text{MoO}_4$  are shown in Figure 1. It is seen that the OCP of Ti in 15 wt% HCl is -0.62 V (vs. SCE) at the very beginning, then gradually decreases with time and stables at -0.66V (vs. SCE). This is mainly due to that the passivation film on Ti surface is gradually destroyed in the HCl solution. The initial OCP of Ti in 15 wt% HCl +0.005 wt%  $\text{Na}_2\text{MoO}_4$  is very close to that in the blank solution, moreover, it shows a similar change tendency to that in the blank solution. However, when the  $\text{Na}_2\text{MoO}_4$  concentration is more than 0.01 wt%, the initial OCP is apparently higher than that in the blank solution. The increase in potential could be ascribed to the formation of a dense passive film on the Ti surface due to strong oxidative properties of molybdates. The OCP of Ti in HCl with 0.01 wt%  $\text{Na}_2\text{MoO}_4$  was -0.18 V (vs. SCE), and it would approach to a positive number when the concentration of  $\text{Na}_2\text{MoO}_4$  exceeds 0.05 wt%. The final stable potentials were as follows: 0.108 V (vs. SCE), 0.157 V (vs. SCE) and 0.118 V (vs. SCE). This suggests that the higher concentration of  $\text{Na}_2\text{MoO}_4$  is, the more protective passive film is.

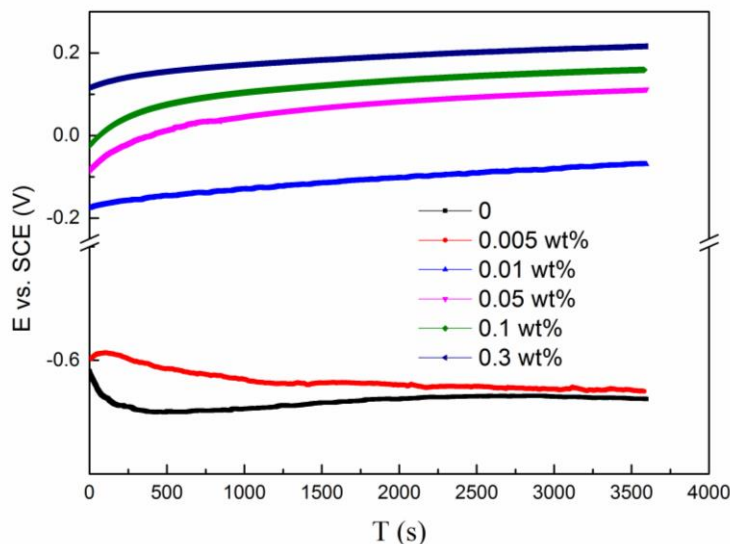


**Figure 1.** The OCP of Ti in deoxygenated 15 wt% HCl solution containing different contents of  $\text{Na}_2\text{MoO}_4$  at 40 °C

### 3.2 Potentiodynamic polarization analysis

Figure 2 shows the potentiodynamic polarization curves of Ti in 15 wt% HCl solution containing different contents of  $\text{Na}_2\text{MoO}_4$ . It can be seen that the linear Tafel region for every anodic side is essentially nonexistent, but it is obviously present at each cathodic side. Therefore, the electrochemical parameters, including corrosion potential ( $E_{corr}$ ), corrosion current density ( $I_{corr}$ ), and cathodic Tafel slope ( $b_c$ ) can be got from Tafel extrapolation of the measured cathodic polarization curves [7].

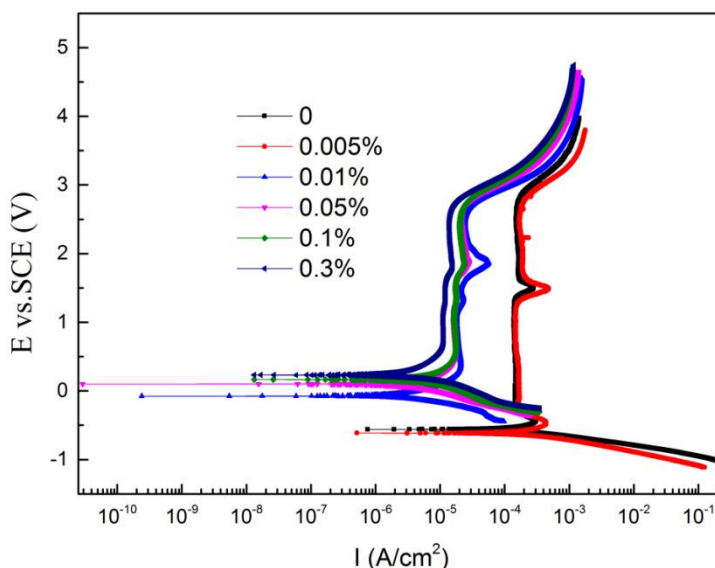


**Figure 2.** Typical polarization curves of Ti in deoxygenated 15 wt% HCl solution containing different contents of  $\text{Na}_2\text{MoO}_4$  at 40 °C

These parameters obtained from Figure 2 and the corresponding inhibition efficiency ( $\eta_i$ ) based on equation (1) are listed in Table 1. The  $I_{corr}$  values and calculated inhibition efficiencies clearly indicate that  $\text{Na}_2\text{MoO}_4$  does not show an good inhibition efficiency when the concentration of  $\text{Na}_2\text{MoO}_4$  is 0.005 wt%, i.e., the inhibition efficiency is only 29.3% in 0.005 wt%  $\text{Na}_2\text{MoO}_4$  solution. However, a good inhibition efficiency can be achieved as the concentration is more than 0.01 wt%. It can be seen that  $I_{corr}$  decreases and inhibition efficiency increases with increasing  $\text{Na}_2\text{MoO}_4$  concentration. 0.01 wt%  $\text{Na}_2\text{MoO}_4$  already provides inhibition efficiency up to 98%. Above this concentration, there is no big change in the inhibition efficiency with the increase of  $\text{Na}_2\text{MoO}_4$  concentration. When  $\text{Na}_2\text{MoO}_4$  concentration increases from 0.01 wt% to 0.3 wt%, the increase in inhibition efficiency is very limited. As listed in Table 1, the  $b_c$  increases with the increasing content of  $\text{Na}_2\text{MoO}_4$  from 0 to 0.05 wt%, indicating that the cathodic reaction is strongly inhibited with the presence of  $\text{Na}_2\text{MoO}_4$ .

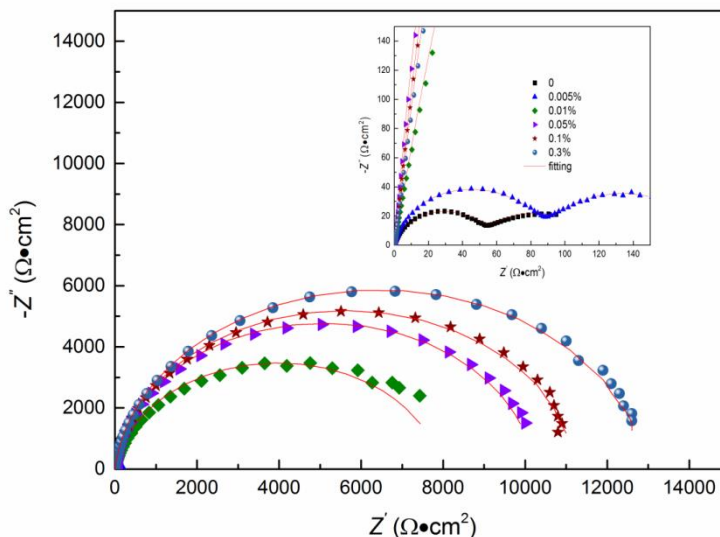
As is shown in Figure 2, typical passivity characteristics can be seen from the anodic polarization curves for the Ti in 15 wt% HCl solutions with and without 0.005 wt%  $\text{Na}_2\text{MoO}_4$ . The anode process of the corrosion reaction changed from active state to passivation state, suggesting that the film of Ti in this environment was less stable, the solution may pass through the passivation film, and the substrate corrosion occurred. However, the anodic potentiodynamic curves of Ti directly reach passivation region when more than 0.01 wt% of  $\text{Na}_2\text{MoO}_4$  was added into the HCl solution, demonstrating that the film in this environment could be stable, which prevented the solution from penetrating the substrate and thus hindered the corrosion of substrate. The anodic oxide film was insoluble or the soluble process was quite slow in the environment, which could isolate the substrate from the solution so that the metal substrate was effectively protected [21].

From the polarization curves, it can be known that molybdate is anodic corrosion inhibitor. As is known that anodic corrosion inhibitors are also known as hazardous corrosion inhibitors. By analyzing the relationship between the concentration of  $\text{Na}_2\text{MoO}_4$  and the corrosion inhibition efficiency, the following conclusions can be drawn: (i) if the concentration of  $\text{Na}_2\text{MoO}_4$  is less than 0.005 wt%, it would accelerate the corrosion of Ti and (ii) there will be dense passive film on Ti surface when the concentration exceeds 0.1wt%, resulting in a good inhibition efficiency.

**Table 1.** Calculated electrochemical parameters from the polarization curves of Ti in deoxygenated 15 wt.% HCl solution containing different contents of  $\text{Na}_2\text{MoO}_4$  at 40 °C

Content of $\text{Na}_2\text{MoO}_4$ (wt%)	$b_c$ (mV dec <sup>-1</sup> )	$I_{corr}$ (A cm <sup>-2</sup> )	$E_{corr}$ (V/SCE)	$\eta\%$
Blank	-133	$2.66 \times 10^{-4}$	-0.601	--
0.005	-180	$1.88 \times 10^{-4}$	-0.656	29.3%
0.01	-241	$4.91 \times 10^{-6}$	-0.076	98.2%
0.05	-241	$2.87 \times 10^{-6}$	0.100	98.9%
0.1	-211	$1.39 \times 10^{-6}$	0.165	99.5%
0.3	-378	$1.11 \times 10^{-6}$	0.234	99.6%

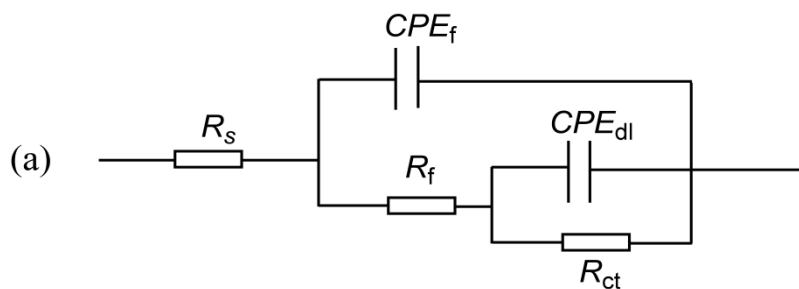
3.3 EIS studies



**Figure 3.** Nyquist plots of EIS data of Ti after 1 h of immersion in deoxygenated 15 wt% HCl solution containing different contents of  $\text{Na}_2\text{MoO}_4$  at 40 °C

Figure 3 presents the EIS spectra obtained for Ti in 15 wt% HCl containing various contents of  $\text{Na}_2\text{MoO}_4$  at open-circuit potential. According to the measured EIS spectra in Figure 3, it can be seen that the radius of the capacitive semicircle increased with increasing concentration of  $\text{Na}_2\text{MoO}_4$ . In order to analyze the corrosion electrochemical mechanism, different models are proposed to fit the EIS data, as is show in Figure 4, where  $R_s$  represents solution resistance between work electrode and reference electrode,  $R_{ct}$  represents charge transfer resistance and  $R_f$  refers the resistance of passive film formed on the Ti electrode surface.

The plots performed two capacitive semicircles at 0.005wt% of  $\text{Na}_2\text{MoO}_4$  or below, indicating that the film is not compact and could not be considered as a homogeneous layer, but a defective layer. At the same time the number of capacitive semicircle varies from two to one. Then the equivalent circuit model in Figure 4a was employed to fit the data. However, when the content of  $\text{Na}_2\text{MoO}_4$  exceeds 0.01 wt%, the plots showed one capacitive semicircle, and the equivalent circuit model in Figure 4b was employed to fit the data. As the content of  $\text{Na}_2\text{MoO}_4$  increases up to 0.01 wt%, the passive film could totally cover the surface of the substrate and supply a good protectiveness. This in good agreement with the polarization curves (Figure 2). As was shown in Figure 3, there was a good agreement between the fitting results and the experimental data.



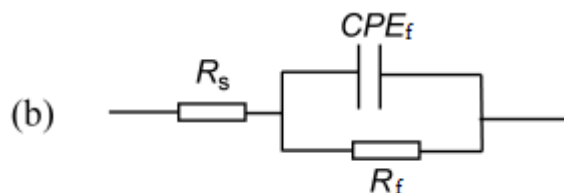


**Figure 4.** Equivalent circuits for Ti in different solution (a):  $\text{Na}_2\text{MoO}_4 \leq 0.005\text{wt}\%$ ; (b)  $\text{Na}_2\text{MoO}_4 \geq 0.01\text{wt}\%$

Table 2 lists the typical fitting parameters (based on circuit depicted in Figure 4). It can be found that the  $CPE_c$  decreases as the increasing concentration of  $\text{Na}_2\text{MoO}_4$ , indicating a decrease in the number or area of defects on the surface film. At the same time, the  $R_c$  increased as the  $\text{Na}_2\text{MoO}_4$  concentration increased, indicating that the protective properties of the surface film were improved obviously.

**Table 2.** Fitting parameters of EIS of Ti in deoxygenated 15 wt% HCl solution containing different contents of  $\text{Na}_2\text{MoO}_4$  at 40 °C

$\text{Na}_2\text{MoO}_4$ content (wt%)	$R_s$ ( $\Omega \text{ cm}^2$ )	$CPE_f$ ( $\text{F cm}^{-2} \text{ Hz}^{1-n_1}$ )	$n_1$	$R_f$ ( $\Omega \text{ cm}^2$ )	$CPE_{dl}$ ( $\text{F cm}^{-2} \text{ Hz}^{1-n_2}$ )	$n_2$	$R_{dl}$ ( $\Omega \text{ cm}^2$ )
0	0.34	1.98e-3	0.86	56.88	9.93e-2	0.84	51.03
0.005	0.34	9.29e-4	0.92	87.41	5.75e-2	0.76	98.7
0.01	0.34	2.73e-4	0.91	7952			
0.05	0.34	1.21e-4	0.96	10200			
0.1	0.34	1.11e-4	0.95	11250			
0.3	0.34	8.83e-5	0.94	12890			

To further understand the inhibition behavior, the EIS spectra of Ti in HCl solution with and without  $\text{Na}_2\text{MoO}_4$  for different immersion times were also presented in Figure 5. It can be seen that the EIS spectra of the Ti in the blank solution varies with immersion time. The impedance increases at the beginning (from 1 h to 72 h) and then decreases. The corresponding parameters fitted by the equivalent circuit (Figure 4a) are also listed in Table 3. According to the fitting results, both  $R_{ct}$  and  $R_f$  first increase and then decrease with time, and the maximum values of both  $R_{ct}$  and  $R_f$  present at 72h of immersion. This is probably due to the formation of a passive film on the Ti surface at the initial immersion stage [7]. However, longer immersion leads to damage of the film, probably because of the development of localized corrosion.

The EIS spectra of the Ti with different immersion times in HCl solution containing 0.01 wt% and 0.3 wt% of  $\text{Na}_2\text{MoO}_4$  are presented in Figure 6 and Figure 7, respectively. The corresponding parameters fitted by the equivalent circuit (Figure 4b) are also listed in Table 4 and Table 5. It should be noted that the impedance of sample immersed in the solution containing different contents of  $\text{Na}_2\text{MoO}_4$  significantly increase in 144 hours, then decrease with time.

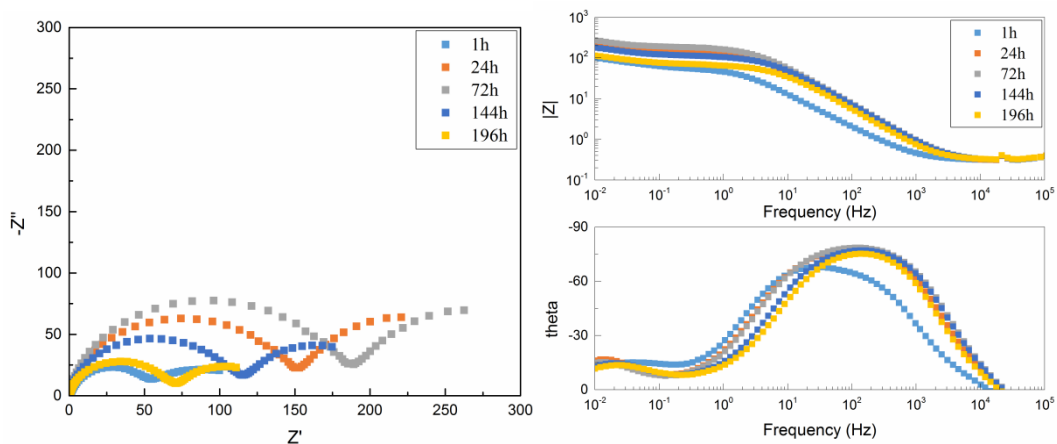


**Figure 5.** EIS data of Ti after different immersion time in deoxygenated 15 wt% HCl solution at 40 °C

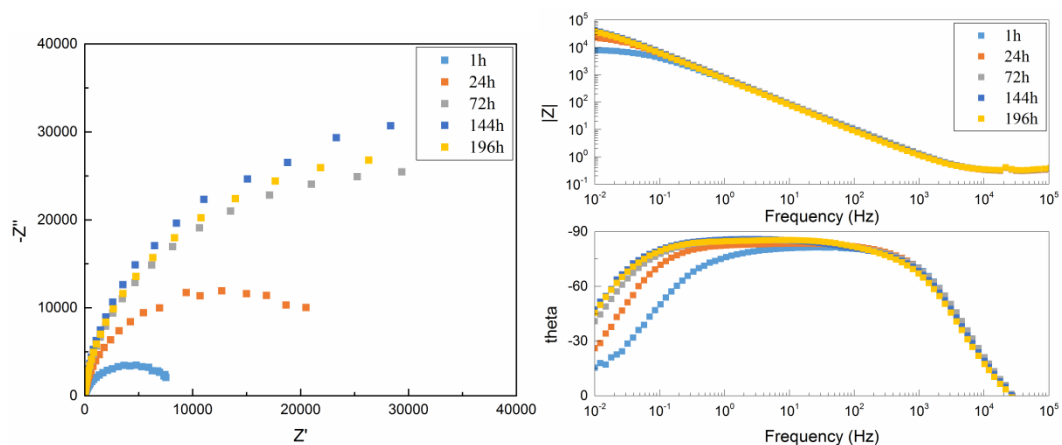


**Figure 6.** EIS data of Ti after different immersion time in deoxygenated 15 wt% HCl solution containing 0.01 wt% Na<sub>2</sub>MoO<sub>4</sub> at 40 °C

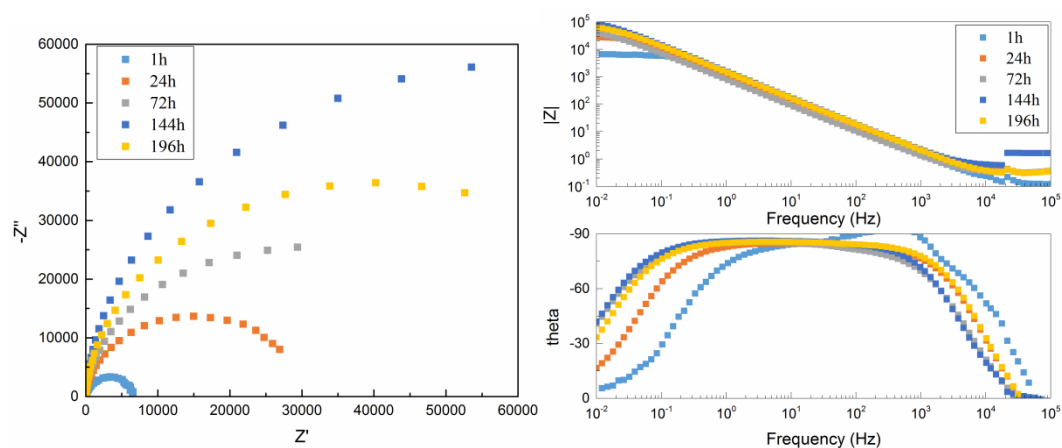


**Figure 7.** EIS data of Ti after different immersion time in deoxygenated 15 wt% HCl solution containing 0.3 wt% Na<sub>2</sub>MoO<sub>4</sub> at 40 °C

**Table 3.** Fitting parameters of EIS of Ti in deoxygenated 15 wt% HCl solution after different immersion times at 40 °C

Time (h)	$R_s$ ( $\Omega \text{ cm}^2$ )	$CPE_f$ ( $\text{F cm}^{-2} \text{ Hz}^{-1-n_1}$ )	$n_1$	$R_f$ ( $\Omega \text{ cm}^2$ )	$CPE_{dl}$ ( $\text{F cm}^{-2} \text{ Hz}^{-1-n_2}$ )	$n_2$	$R_{dl}$ ( $\Omega \text{ cm}^2$ )
1	0.34	1.98e-3	0.86	56.88	9.93e-2	0.84	51.03
6	0.3058	8.083E-4	0.87	95.33	0.067	0.82	102.6
24	0.3021	4.684E-4	0.92	145.7	0.0589	0.74	216.5
72	0.3066	3.484E-4	0.92	175.9	0.0437	0.64	332
96	0.3057	3.471E-4	0.93	166.6	0.0406	0.61	392.3
144	0.307	3.689E-4	0.92	105.1	0.045	0.59	186.3
192	0.3153	4.801E-4	0.92	62.39	0.057	0.54	117.7

**Table 4.** Fitting parameters of EIS of Ti in deoxygenated 15 wt% HCl solution containing 0.01 wt%  $\text{Na}_2\text{MoO}_4$  after different immersion times at 40 °C.

Time (h)	$R_s$ ( $\Omega \text{ cm}^2$ )	$CPE_f$ ( $\text{F cm}^{-2} \text{ Hz}^{-1-n_1}$ )	$n_1$	$R_f$ ( $\Omega \text{ cm}^2$ )
1	0.2951	2.796E-4	0.91	8108
6	0.3009	2.299E-4	0.93	16910
24	0.3016	2.493E-4	0.93	26440
48	0.3135	2.451E-4	0.95	38180
72	0.3201	2.211E-4	0.94	54910
96	0.3297	2.323E-4	0.94	62870
120	0.3316	2.422E-4	0.96	64860
144	0.3264	2.396E-4	0.94	67870
192	0.3328	2.527E-4	0.94	58850

**Table 5.** Fitting parameters of EIS of Ti in deoxygenated 15 wt HCl% solution containing 0.3 wt%  $\text{Na}_2\text{MoO}_4$  after different immersion times at 40 °C.

Time (h)	$R_s$ ( $\Omega \text{ cm}^2$ )	$CPE_f$ ( $\text{F cm}^{-2} \text{ Hz}^{-1-n_1}$ )	$n_1$	$R_f$ ( $\Omega \text{ cm}^2$ )
1	0.3325	1.138E-4	0.98	6537
6	0.323	1.222E-4	0.97	13230
24	0.3121	1.293E-4	0.95	29990
48	0.3067	1.194E-4	0.95	50820
72	0.3065	1.187E-4	0.96	58770
120	0.3032	1.051E-4	0.96	113300
144	0.5776	1.079E-4	0.96	120100
168	0.3	1.127E-4	0.96	108640
192	0.2986	1.164E-4	0.95	97990

The most important observation from these data is the change in EIS characteristics. The EIS spectra clearly show two capacitive loops in the blank solution, but after addition of molybdate, the two-capacitive-loop feature becomes insignificant with the immersion time because the phase angle at

the high frequency increases. Besides, the impedance at the high frequency range corresponding to the surface corrosion products also increases with the immersion time, suggesting that the inhibitors might have led to a change in compactness of the film on the Ti surface.

### 3.4 Surface morphology and composition

Figure 8 shows SEM surface morphologies of Ti after 3 days of immersion in the blank and  $\text{Na}_2\text{MoO}_4$  containing solutions at  $40^\circ\text{C}$ . It can be seen that in the absence of molybdate, honeycomb-shaped surface morphologies are present on its surface. However, after addition of various concentrations of  $\text{Na}_2\text{MoO}_4$ , the surface of Ti is still smooth and some fine streaks originated from the grinding process can still be found. This indicates that the addition of  $\text{Na}_2\text{MoO}_4$  inhibitor may result in formation of a dense film on the Ti surface, providing a good protectiveness for Ti.

The surface composition of Ti in deoxygenated 15 wt% HCl solution and in HCl solution containing 0.1 wt%  $\text{Na}_2\text{MoO}_4$  for 72 h at  $40^\circ\text{C}$  are also shown in Figure 9. The detected elements mainly include Ti and Cl. However, a small amount of oxygen is detected, indicating the passivation film is extremely thin.

Figure 10 shows the surface composition of Ti in HCl solution containing 0.1 wt%  $\text{Na}_2\text{MoO}_4$  for 72 h at  $40^\circ\text{C}$ . Compared with Fig. 9, it can be seen that the surface of Ti distributed a lot of oxygen, suggesting there is a denser passivation film.

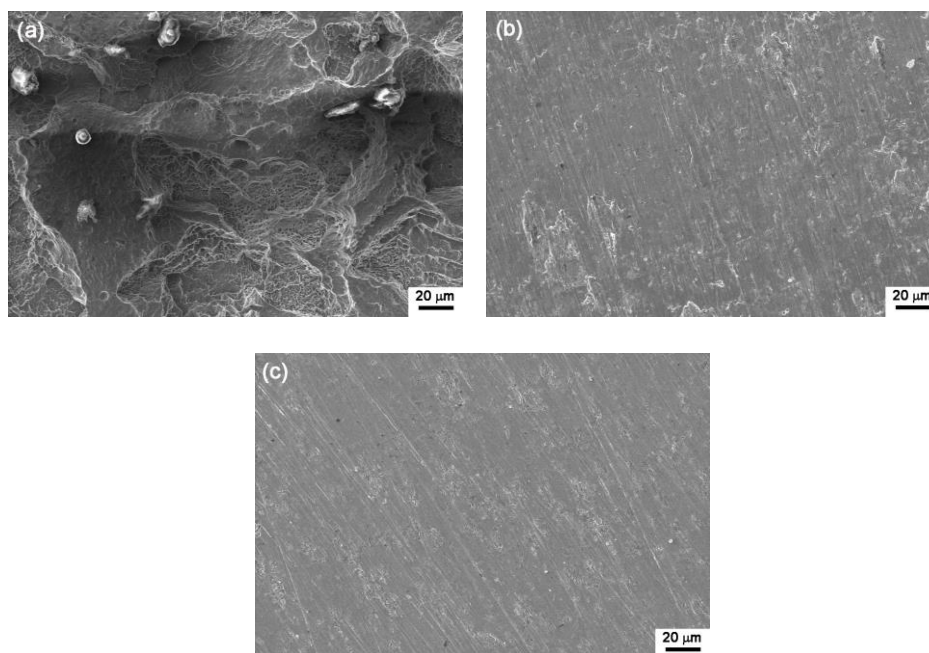


**Figure 8.** SEM images of Ti after 72 h of immersion in deoxygenated 15 wt% HCl solution containing various contents of  $\text{Na}_2\text{MoO}_4$  (a) 0, (b) 0.01wt% and (c) 0.3 wt% at  $40^\circ\text{C}$ .

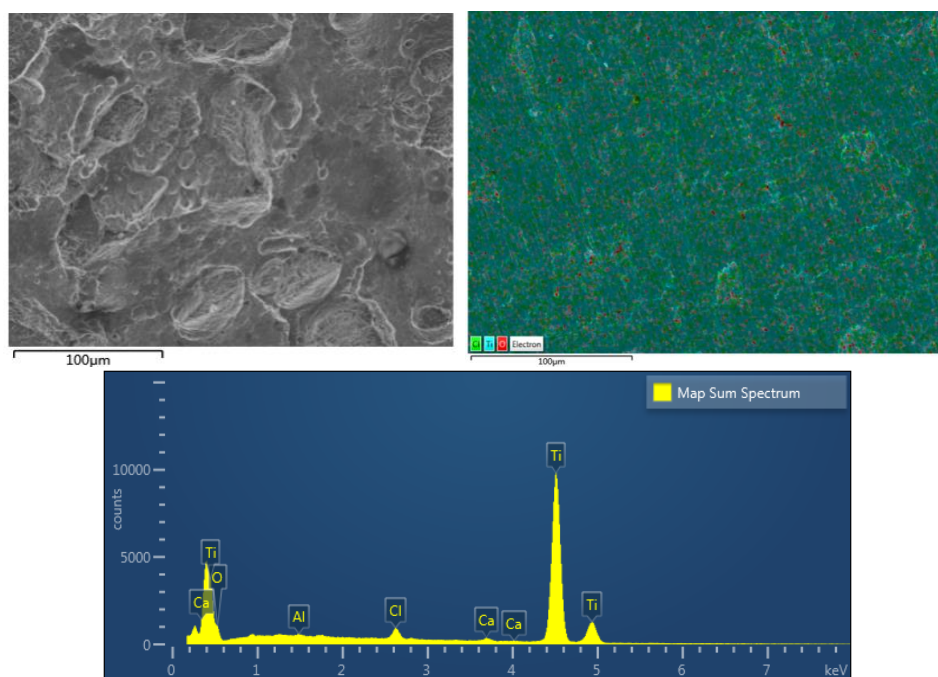


**Figure 9.** EDS of Ti after 72 h of immersion in deaerated 15 wt% HCl solution at 40 °C

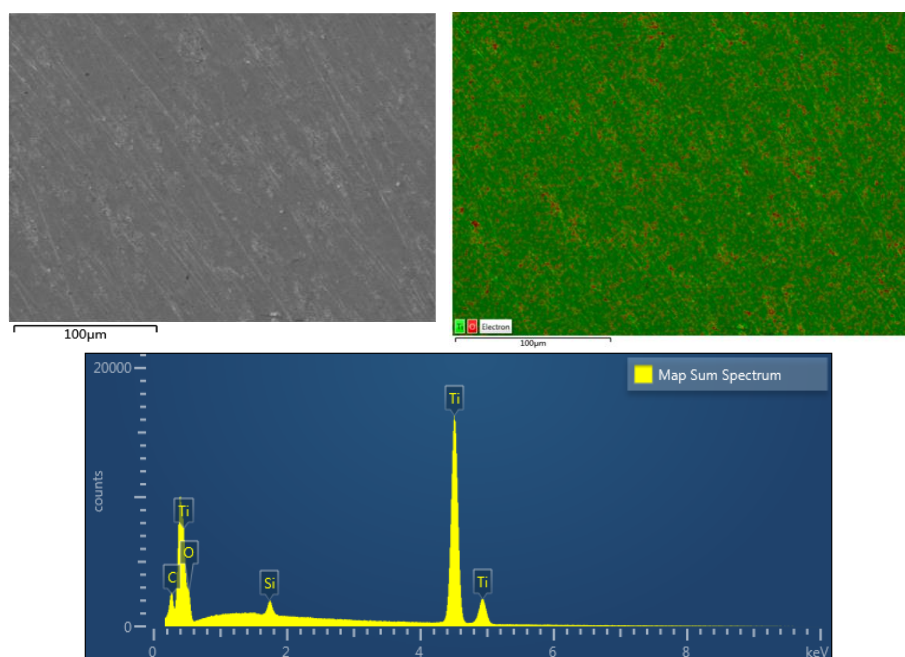


**Figure 10.** EDS of Ti after 72 h of immersion in deaerated 15 wt% HCl solution containing 0.1 wt%  $\text{Na}_2\text{MoO}_4$  at 40 °C

### 3.5 Mott–Schottky analysis

The Mott-Schottky equations to describe the  $C_{sc}^{-2}$  as a function of the potential are as follows [22]:

$$\text{For n type semiconductor: } \frac{1}{C_{sc}^2} = \frac{2}{\epsilon\epsilon_0 e N_D} \left( E - E_{fb} - \frac{kT}{e} \right) \quad (2)$$

$$\text{For p type semiconductor: } \frac{1}{C_{sc}^2} = \frac{-2}{\epsilon\epsilon_0 e N_A} \left( E - E_{fb} - \frac{kT}{e} \right) \quad (3)$$

where  $C_{sc}$  is the space-charge capacitance,  $N_D$  and  $N_A$  are donor and acceptor densities ( $\text{cm}^{-3}$ ),  $e$  is the electron charge,  $\epsilon$  is the dielectric constant of Ti oxide ( $\epsilon = 55$ ) [23],  $\epsilon_0$  is the vacuum permittivity ( $8.854 \times 10^{-14}$  F/cm),  $k$  is the Boltzmann constant ( $1.38 \times 10^{-23}$  J/K),  $T$  is the absolute temperature and  $E_{fb}$  is the flat band potential (obtained from the extrapolation to  $C_{sc}^{-2} = 0$ ).

The Mott–Schottky plots display the  $C^{-2}$  versus  $E$  for the passive film formed in different environments at open circuit potential, as is shown in Figure 11. Table 6 shows the calculated donor densities of the film formed in different solution, respectively. From the Table 6, it can be known that the orders of magnitude are  $10^{21}/\text{cm}^3$ , it could be concluded that the passive film was highly disordered. Changes in  $N_D$  concentration corresponded to the carrier concentration in the semiconductor, which consisted of oxygen vacancies and cation interstitials imparting n-type character. With the addition of  $\text{Na}_2\text{MoO}_4$ , the defect density had a little change. This could be due to the decline in the affinity of absorption or adsorption of  $\text{H}^+$  cations on the passive film, which made hydrogen evolution reaction more difficult, as shown in polarization curves (Figure 1).

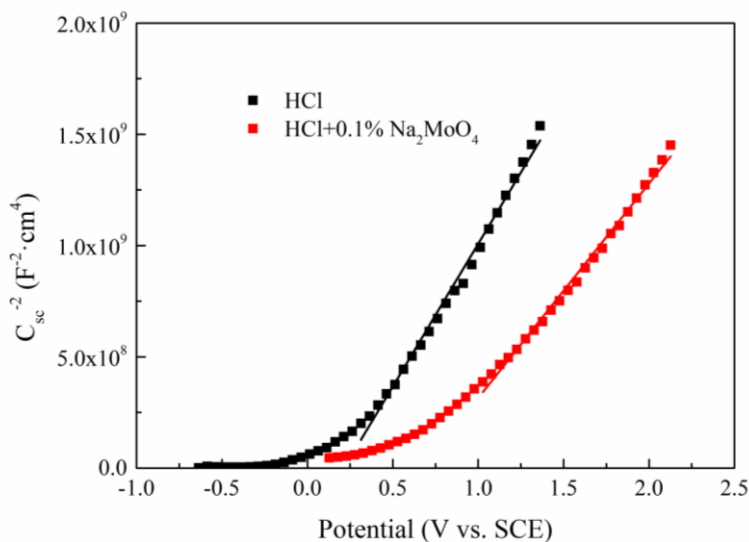


**Figure 11.** Mott-schottky approach for film formed on Ti in deaerated 15 wt% HCl solution and containing 0.1 wt%  $\text{Na}_2\text{MoO}_4$  at 40 °C

**Table 6.** Effect of  $\text{Na}_2\text{MoO}_4$  on semiconducting properties of passive film formed on Ti in deaerated 15 wt% HCl solution

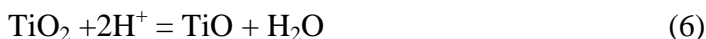
Solution environment	$N_D, \text{cm}^{-3}$	$k$
HCl	$1.82 \times 10^{21}$	$9.64 \times 10^8$
HCl+0.1 wt% $\text{Na}_2\text{MoO}_4$	$2.66 \times 10^{21}$	$1.28 \times 10^9$

### 3.6 Mechanism analysis

In 15 wt% HCl, the cathode reaction is:



Combining the electrochemical experimental results with the SEM analysis, a reasonable conclusion can be inferred that when the concentration of  $\text{Na}_2\text{MoO}_4$  is not more than 0.0005 M, the main anodic reactions are [24]:



Equation (5) represents the electrochemical generation of oxide film, Equation (6) represents the chemical dissolution of oxide film, and Equation (7) represents the chemical dissolution of Ti. When the concentration of  $\text{Na}_2\text{MoO}_4$  in 15 wt% HCl is 0.01 wt% or above, the main anodic reaction is [25]:



Accordingly, a  $\text{TiO}_2$  film which can supply a good protectiveness for Ti can be formed in the presence of molybdate.

## 4. CONCLUSIONS

The electrochemical behaviors of Ti in 15 wt% HCl solutions at different concentrations of  $\text{Na}_2\text{MoO}_4$  were studied by polarization curves, EIS, Mott–Schottky, and SEM coupled with EDS. The main conclusions can be drawn as follows:

(1) The OCP of Ti in 15 wt% HCl solution increases with the increasing of  $\text{Na}_2\text{MoO}_4$  content. The polarization curves revealed that the hydrogen evolution reaction (cathodic process) was remarkably inhibited, and the anode process of the corrosion reaction changed from active-passivation state to passivation state when the content of  $\text{Na}_2\text{MoO}_4$  exceeded 0.01 wt%.

(2) EIS showed that the capacitive semicircle varies from two to one, with a remarkable increase of the impedance values after the content of  $\text{Na}_2\text{MoO}_4$  increased up to 0.01 wt%.

(3) The EDS results indicated that the content of oxygen element in the passivation film increased significantly when 0.01 wt%  $\text{Na}_2\text{MoO}_4$  was added into the solution.

## ACKNOWLEDGEMENTS

The authors thank the financial supports of Open Fund of State Key Laboratory of Oil and Gas Reservoir Geology and Exploitation (Southwest Petroleum University) (grant number PLN1308) and National Natural Science Foundation of China (grant number 51501160).

## References

1. M. Chellappa and U. Vijayalakshmi, *Mater. Sci. Eng. C*, 71 (2017) 879.

2. A.M. Al-Mayouf, A.A. Al-Swayih, N.A. Al-Mobarak and A.S. Al-Jabab, *Mater. Chem. Phys.*, 86 (2004) 320.
3. B.J. Zhao, H. Wang, N. Qiao, C. Wang and M. Hu, *Mater. Sci. Eng. C*, 70 (2017) 832.
4. Y. Bai, Y.L. Hao, S.J. Li, Y.Q. Hao, R. Yang and F. Prima, *Mater. Sci. Eng. C*, 33 (2013) 2159.
5. M.J. Jackson, J. Kopac, M. Balazic, D. Bombac, M. Brojan and F. Kosei, Ti and Ti alloy applications in medicine, in: W. Ahmed and M.J. Jackson, (Eds.), *Surgical tools and medical devices*. Springer International Publishing, (2016) Switzerland.
6. A.R. Rafieerad, M.R. Ashra, R. Mahmoodian and A.R. Bushroa, *Mater. Sci. Eng. C*, 57 (2015) 397.
7. X. Zhong, S. Yu, J. Hu, L. Chen, Y. Shi, S. Gao, Z. Zhang, D. Zeng and T. Shi, *Int. J. Electrochem. Sci.*, 12 (2017) 2875.
8. A. M. Al-Mayouf, A. A. Al-Swayih, N. A. Al-Mobarak, *Mater. Corros.*, 55 (2004) 88.
9. B. Chambers, A. Venkatesh and S. Mishael, Performance of tantalum-surface alloy on stainless steel and multiple corrosion resistant alloys in laboratory evaluation of deep well acidizing environments. NACE Corrosion 2011 Conference & Expo, Houston, USA, 2011, Paper No. 11106.
10. Z. Su, M. Bühl and W. Zhou, *J. Am. Chem. Soc.*, 131 (2009) 8697.
11. R.D. Kane, S. Srinivasan, B. Craig and K.M. Yap, A comprehensive study of Ti alloys for high pressure (HPHT) wells. NACE Corrosion 2015 Conference & Expo, Dallas, USA, 2015, Paper No. 5512.
12. R.W. Schutz and B.C. Jena, Sour service test qualification of a new high-strength Ti alloy-UNS R55400. NACE Corrosion 2015 Conference & Expo, Dallas, USA, Paper No. 5794.
13. J.A. Petit, G. Chatainier and F. Dabosi, *Corros. Sci.*, 21 (1981) 279.
14. A.S. Mogoda, Y.H. Ahmad and A. Badawy, *Mater. Corros.*, 55 (2004) 449.
15. I.N. Andijani, S. Ahmad and A.U. Malik, *Desalination*, 129 (2000) 45.
16. P.R. Shibad, J. Balachandra and M. Division, *Anti-Corrosion*, 16 (1976) 16.
17. T.-P. Cheng, J.-T. Lee and W.-T. Tscai, *Electrochim. Acta*, 36 (1991) 2069.
18. X. Zhang, L. Chen, B. Medgyes, Z. Zhang, S. Gao and L. Jakab, *RSC Adv.*, 7 (2017) 28186.
19. F. Contu, B. Elsener and H. Böhni, *Corros. Sci.* 46 (2004) 2241.
20. X. Zhong, S. Yu, L. Chen, J. Hu and Z. Zhang, *J. Mater Sci: Mater. Electron.*, 28 (2017) 2279.
21. L. Wang, X.Q. Cheng, S.J. Gao, X.G. Li, and S.W. Zou, *Mater. Corros.*, 66 (2015) 251.
22. C.S. Enache, J. Schoonman and R. van Krol, *J. Electroceram.*, 13 (2004) 177.
23. M. C. K. Sellers and E. G. Seebauer, *Thin Solid Films*, 519 (2011) 2103.
24. J. H. Du, *Rare Metal Mater. Eng.*, 21 (1992) 27.
25. A. S. Mogoda, Y. H. Ahmad and W. A. Badawy, *Mater. Corros.*, 55 (2004) 449.